

A NEW APPROACH TO CONSTRAIN BLACK HOLE SPINS IN ACTIVE GALAXIES USING OPTICAL REVERBERATION MAPPING

JIAN-MIN WANG^{1,2}, PU DU¹, YAN-RONG LI¹, LUIS C. HO^{3,4}, CHEN HU¹, AND JIN-MING BAI⁵

Received 2014 July 8; accepted 2014 August 6

ABSTRACT

A tight relation between the size of the broad-line region (BLR) and optical luminosity has been established in about 50 active galactic nuclei studied through reverberation mapping of the broad H β emission line. The $R_{\text{BLR}} - L$ relation arises from simple photoionization considerations. Using a general relativistic model of an optically thick, geometrically thin accretion disk, we show that the ionizing luminosity jointly depends on black hole mass, accretion rate, and spin. The non-monotonic relation between the ionizing and optical luminosity gives rise to a complicated relation between the BLR size and the optical luminosity. We show that the reverberation lag of H β to the varying continuum depends very sensitively to black hole spin. For retrograde spins, the disk is so cold that there is a deficit of ionizing photons in the BLR, resulting in shrinkage of the hydrogen ionization front with increasing optical luminosity, and hence shortened H β lags. This effect is specially striking for luminous quasars undergoing retrograde accretion, manifesting in strong deviations from the canonical $R_{\text{BLR}} - L$ relation. This could lead to a method to estimate black hole spins of quasars and to study their cosmic evolution. At the same time, the small scatter of the observed $R_{\text{BLR}} - L$ relation for the current sample of reverberation-mapped active galaxies implies that the majority of these sources have rapidly spinning black holes.

Subject headings: galaxies: active – black holes: accretion

1. INTRODUCTION

The broad emission lines from quasars and active galactic nuclei (AGNs) largely reflect virial motions of broad-line region (BLR) clouds governed by the gravitational potential of the central supermassive black hole (BH). The BLR clouds are mainly photoionized by the continuum emission from the accretion disk (e.g., Osterbrock & Mathews 1986; Ho 2008), and the detailed emission-line spectra depend, at least in part, on the spectral energy distribution (SED) of the disk. The SED, in turn, varies as a function of BH mass, spin, and accretion rate.

Reverberation mapping (RM; Blandford & McKee 1982) of ~ 50 AGNs has discovered a very tight correlation between BLR size, as measured from the H β lag in response to the varying continuum, and the optical luminosity (popularly measured at 5100 Å; Kaspi et al. 2000; Bentz et al. 2013). This well-known relation can be described as $R_{\text{BLR}} \approx 36.3 L_{44}^{\gamma} \text{ld}$, where $\gamma = 0.546_{-0.027}^{+0.027}$ and L_{44} is the 5100 Å luminosity L_{5100} in units of $10^{44} \text{erg s}^{-1}$. This is a natural consequence of photoionization of BLR clouds. Defining the ionisation parameter as $U = Q_{\text{ion}}/4\pi R_{\text{H}\beta}^2 c n_e$, with n_e the electron density, Q_{ion} the rate of ionizing photons, and c the speed of light, this empirical $R_{\text{BLR}} - L$ relation can be explained if the photoionized clouds obey the condition $n_e U \sim 10^{10}$ (Negrete et al. 2013). Alternatively, sublimation of dust particles and energy balance between heating and radiation loss in the

BLR produces a similar scaling relation between R_{BLR} and L (Netzer & Laor 1993). In either case, this observational relation sets strong constraints on the physical properties of the BLR. It is of interest to explore how the $R_{\text{BLR}} - L$ is affected by the ionizing SED.

In this Letter, we show that ionizing luminosity L_{ion} is a complicated function of BH mass, spin, and accretion rate. It can be much fainter than L_{5100} , and thus the H β -emitting region can be much smaller than that predicted by the $R_{\text{BLR}} - L_{5100}$ relation, which is based on L_{5100} . We emphasize the influence of BH mass and spin on the SED, and thus on H β reverberation. The sensitivity of H β lags to BH spin provides a promising method to estimate spins from RM observations.

2. IONIZING LUMINOSITY FROM ACCRETION DISKS

2.1. Emissions from Accretion Disks

We employ the general relativistic version of the Shakura-Sunyaev (1973) disk (Page & Thorne 1974). General relativistic effects are important because the ionizing photons are emitted from regions very close to the innermost last stable orbit (r_{ms}), especially for extremely massive BHs ($\sim 10^9 M_{\odot}$). We define the dimensionless accretion rate as $\dot{m} = 0.1 \dot{M}_{\bullet} c^2 / L_{\text{Edd}}$, where \dot{M}_{\bullet} is the accretion rate, $L_{\text{Edd}} = 4\pi G M_{\bullet} m_p c / \sigma_T$ is the Eddington luminosity, M_{\bullet} is the BH mass, σ_T is the Thompson cross section, and G is the gravitation constant. Disks with accretion rates $\dot{m} \approx 0.01 - 0.3$ are in the Shakura-Sunyaev regime, characterized by being geometrically thin and optically thick. Above this regime in \dot{m} , accretion onto BHs is described by slim disks (Abramowicz et al. 1988). Wang et al. (2014) recently discuss the influence of slim disks on the BLR. This paper is devoted to thin disks. The radiation flux from the disks is given by

$$F = \frac{3m_p c^5}{2\sigma_T G M_{\bullet}} \frac{\dot{m}}{r^3} f_{\text{GR}}(r, a) \quad (1)$$

$$= 6.86 \times 10^{17} \dot{m}_{0.1} M_9^{-1} r^{-3} f_{\text{GR}}(r, a) \text{ erg s}^{-1} \text{ cm}^{-2},$$

¹ Key Laboratory for Particle Astrophysics, Institute of High Energy Physics, Chinese Academy of Sciences, 19B Yuquan Road, Beijing 100049, China.

² National Astronomical Observatories of China, Chinese Academy of Sciences, 20A Datun Road, Beijing 100020, China

³ Kavli Institute for Astronomy and Astrophysics, Peking University, Beijing 100875, China

⁴ Department of Astronomy, Peking University, Beijing 100875, China

⁵ Yunnan Observatory, Chinese Academy of Sciences, Kunming 650011, China

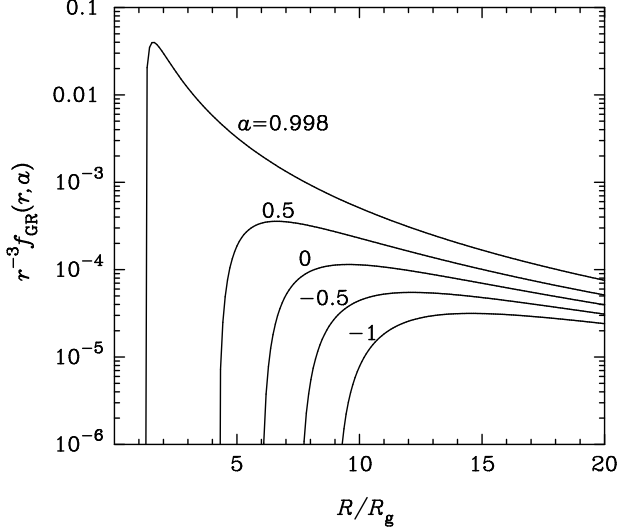


FIG. 1.— The function $r^{-3} f_{\text{GR}}(r, a)$, for $a = 0.998$ to $a = -1$. Two characteristics can be seen: (1) the last stable inner radii are different for $a = 0.998$ and $a = -1$, and hence the total dissipated energy and SED are very different; (2) the function tends to r^{-3} when $r \rightarrow \infty$, which leads to similar optical radiation (e.g., at 5100 \AA) for $a = \pm 1$.

where $\dot{m}_{0.1} = \dot{m}/0.1$, a is the specific angular momentum of the BH, $M_9 = M_\bullet/10^9 M_\odot$, $r = R/R_g$ is the dimensionless radius, and $R_g = GM_\bullet/c^2 = 1.48 \times 10^{14} M_9 \text{ cm}$. Here, $f_{\text{GR}}(r, a)$ is a factor that includes general relativistic effects (Page & Thorne 1974):

$$f_{\text{GR}}(r, a) = \frac{1}{C\sqrt{r}} \left\{ \sqrt{r} - \sqrt{r_{\text{ms}}} - \frac{3a}{4} \ln \frac{r}{r_{\text{ms}}} - 3 \left[\frac{(x_1 - a)^2}{x_1(x_1 - x_2)(x_1 - x_3)} \right. \right. \\ \times \ln \frac{\sqrt{r} - x_1}{\sqrt{r_{\text{ms}}} - x_1} + \frac{(x_2 - a)^2}{x_2(x_2 - x_1)(x_2 - x_3)} \ln \frac{\sqrt{r} - x_2}{\sqrt{r_{\text{ms}}} - x_2} \\ \left. \left. + \frac{(x_3 - a)^2}{x_3(x_3 - x_1)(x_3 - x_2)} \ln \frac{\sqrt{r} - x_3}{\sqrt{r_{\text{ms}}} - x_3} \right] \right\}, \quad (2)$$

where $C = 1 - 3/r + 2a/r^{3/2}$, $x_1 = 2 \cos[(\Theta_a - \pi)/3]$, $x_2 = 2 \cos[(\Theta_a + \pi)/3]$, $x_3 = -2 \cos(\Theta_a/3)$, and $\Theta_a = \arccos a$. Here r_{ms} is the last stable orbit, and can be expressed by $r_{\text{ms}} = [3 + Z_2 \mp \sqrt{(3 - Z_1)(3 + Z_1 + 2Z_2)}]$, $Z_1 = 1 + (1 - a^2)^{1/3} [(1 + a)^{1/3} + (1 - a)^{1/3}]$ and $Z_2 = \sqrt{3a^2 + Z_1^2}$. Figure 1 shows the function $r^{-3} f_{\text{GR}}(r, a)$, which is related to the effective temperature of the disk, for different spins. We find that the peak of the dissipation rate is sensitive to a , lending us an opportunity to constrain the spin.

The SED is governed by the effective temperature distribution of the disk, which follows from $T_{\text{eff}} = [F(r)/\sigma_{\text{SB}}]^{1/4}$, where σ_{SB} is the Stefan-Boltzmann constant,

$$T_{\text{eff}} = 3.32 \times 10^5 \dot{m}_{0.1}^{1/4} M_9^{-1/4} r^{-3/4} f_{\text{R}}^{1/4} \text{ K}, \quad (3)$$

and can be obtained by integrating the entire disk from r_{ms} to infinity,

$$L_\nu = 32\pi^2 \cos i R_g^2 \int_{r_{\text{ms}}}^{\infty} \frac{2h}{c^2} \frac{\nu^3 r dr}{e^{h\nu/kT_{\text{eff}}} - 1}, \quad (4)$$

where h and k are the Planck and Boltzmann constants, respectively, and i is the inclination of the disk with respect to the line of sight. For a given wavelength $\lambda = c/\nu$, we have the

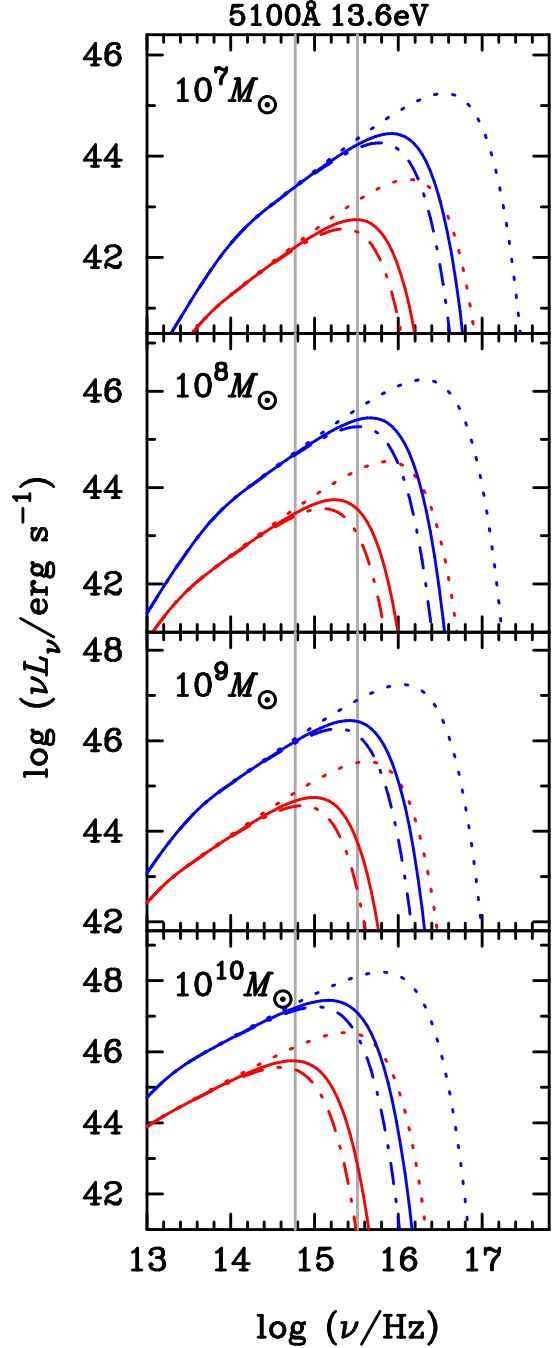


FIG. 2.— The SEDs of accretion disks and their dependence on BH mass, accretion rate, and BH spin. The blue and red curves are for $\dot{m} = 0.5$ and 0.01 , and the dashed-dotted, solid, and dotted lines are for spin $a = -1, 0$, and 0.998 , respectively. The two grey vertical lines mark 5100 \AA and 13.6 eV .

luminosity $L_\lambda = \nu L_\nu$, which is used for the empirical correlation with the BLR size. Integration of Equation (4) yields the approximate functional form $L_\nu \propto \nu^{1/3}$. For convenience, we set $\cos i = 1$.

Figure 2 shows spectra from accretion disks with different parameters. We keep the accretion rates in the Shakura-Sunyaev regime in order to avoid the self-shadowing effects of the disk itself (Wang et al. 2014). For the same \dot{m} , retrograde spins produce much softer SEDs than prograde spins. For each disk with (M_\bullet, \dot{m}) , we plot spins of $a = -1, 0$, and

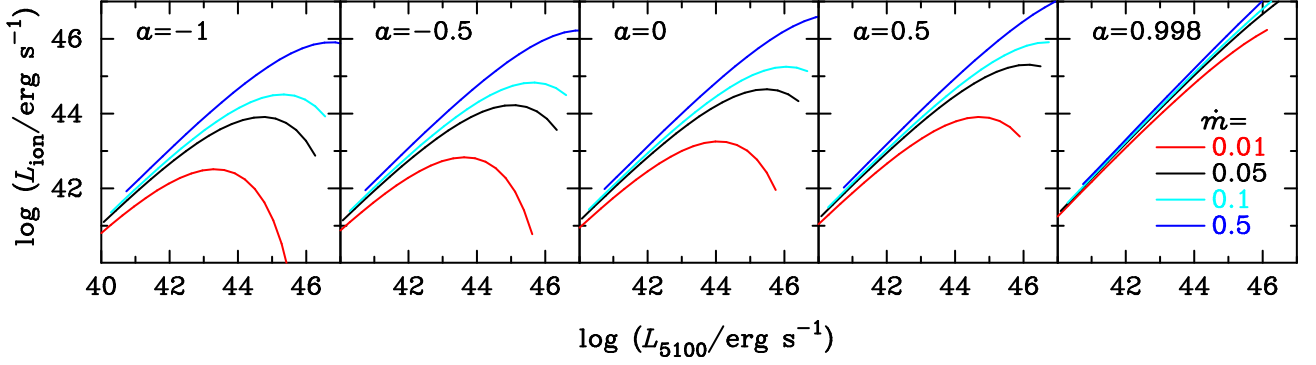


FIG. 3.— Relation between the hydrogen ionizing luminosity and the luminosity at 5100 Å. Panels from left to right are for different values of BH spin, from $a = -1.0$ to $a = 0.998$. Each panel plots four colour lines for different accretion rates. Given \dot{m} and a , L_{5100} is a function of the BH mass.

0.998. We find the following. (1) The luminosity at 5100 Å, L_{5100} , is always insensitive to spin for $\dot{m} = 0.5$ to 0.01, except for extremely large BHs with $M_\bullet \gtrsim 10^{10} M_\odot$. (2) For a given \dot{m} , the SED is very sensitive to a , except for values of $a = 0$ or $a = -1$. (3) For $M_\bullet \lesssim 10^8 M_\odot$ and higher accretion rate ($\dot{m} \gtrsim 0.5$), the hydrogen ionizing luminosity depends very little on spin ($\Delta \log L_{13.6\text{eV}} \lesssim 0.5$ dex for $a = 0.998$ and $a = -1$); thus, the present approach of constraining spins is not effective for less massive BHs (see discussion in §2.2).

2.2. Photoionizing Luminosity

The ionizing portion of the SED is sensitive to (M_\bullet, \dot{m}, a) . Integration of the SED above $\epsilon_1 = 13.6$ eV yields the ionizing luminosity. To estimate the number of ionizing photons, we need to know the photoionization cross section of hydrogen (e.g., Osterbrock 1989). For $h\nu \geq \epsilon_1$,

$$\sigma_\nu = 6.3 \times 10^{-18} \left(\frac{\epsilon_1}{h\nu} \right)^4 \frac{e^{4 - [(4 \tan^{-1} \epsilon)/\epsilon]}}{1 - e^{-2\pi/\epsilon}} \text{ cm}^2, \quad (5)$$

where $\epsilon = (h\nu/\epsilon_1 - 1)^{1/2}$, h is the Planck constant; otherwise, $\sigma_\nu = 0$ when $h\nu < \epsilon_1$. The total luminosity to ionise hydrogen is

$$L_{\text{ion}} = \frac{\int_{\epsilon_1}^{\infty} \nu L_\nu \sigma_\nu d\nu}{\int_{\epsilon_1}^{\infty} \sigma_\nu d\nu}. \quad (6)$$

The observed $\text{H}\beta$ luminosity is given by $L_{\text{H}\beta} = (\Delta\Omega/4\pi)(\epsilon_{\text{H}\beta}/\alpha_B)Q_{\text{ion}}(\text{H}^0)$, where $\Delta\Omega$ is the solid angle subtended by the BLR, $\epsilon_{\text{H}\beta}$ is the recombination-line emission coefficient of $\text{H}\beta$, α_B is the radiative recombination coefficient for hydrogen quantum levels $n = 2$ and higher, $Q_{\text{ion}}(\text{H}^0)$ is the ionizing photon rate. In principle, the $\text{H}\beta$ luminosity ($L_{\text{H}\beta}$) emitted from the photoionized clouds in the BLR is proportional to L_{ion} , but it also depends on some details of the clouds and the BLR. The $L_{\text{H}\beta} - L_{5100}$ relation can be used to observationally test photoionization processes.

Figure 3 shows predicted $L_{\text{ion}} - L_{5100}$ relations for disks with $a = (-1, -0.5, 0, 0.5, 0.998)$ and $\dot{m} = (0.01, 0.1, 0.5)$. The ratio $\ell = L_{\text{ion}}/L_{5100}$ is a complicated function of (M_\bullet, \dot{m}, a) . For a given a and \dot{m} , L_{5100} increases with BH mass, approximately as $L_{5100} \propto M_\bullet^{1/3}$ for a Newtonian potential. For the case of $a = -1$ (left panel of Fig. 3), we find that L_{ion} linearly increases with L_{5100} in logarithmic space until a critical luminosity L_{5100}^c . Above L_{5100}^c , L_{ion} decreases exponentially with L_{5100} . This means that L_{ion} does not follow a linear relation with the observed optical luminosity. L_{5100}^c is jointly determined by \dot{m} and a , increasing with increasing a . For ex-

treme prograde spins, the $L_{\text{ion}} - L_{5100}$ relation remains linear for $\dot{m} \gtrsim 0.01$ up to $L_{5100} \approx 10^{47} \text{ erg s}^{-1}$, which corresponds to the most massive BHs in quasars ($\sim 10^{10} M_\odot$). The non-monotonic connection between L_{ion} and L_{5100} has strong observational implications for the BLR as well as BH spins.

We note that the $L_{\text{ion}} - L_{5100}$ relation discussed here is closely related to the well-known correlation between Balmer line luminosity and optical continuum, which is usually taken as evidence for photoionization (e.g., Shuder 1981; Greene & Ho 2005). However, for the comparison between $\text{H}\beta$ and 5100 Å continuum, the rms scatter of either the luminosity-luminosity or flux-flux correlations is still $\sim 0.2 - 0.3$ dex, depending on the sample and method of spectral analysis (Greene & Ho 2005; Hu et al. 2008; Shen et al. 2011). The scatter might reflect the range in BLR covering factors of individual objects, or, alternatively, variations in M_\bullet , \dot{m} , and a .

The AGN continuum is composed of optical-UV blackbody radiation from the cold disk (the “big blue bump”) and Comptonization of the disk photons into X-rays by a hot corona above the disk (e.g., Haardt & Maraschi 1991). The fraction (f_c) of the gravitational energy dissipated in the hot corona is anti-correlated with \dot{m} (see Fig. 1b in Wang et al. 2004), but it remains the largest source of uncertainty in the disk-corona system (e.g., Svensson & Zdziarski 1994). In principle, f_c should be determined by the details of the accretion physics, such as the radial motion of the accretion flow, the magnetic field, and its reconnection (e.g., Merloni & Fabian 2002; Wang et al. 2004; Cao 2009; Done et al. 2013; Uzdensky 2013). Observations show that the maximum value of f_c is $\lesssim 0.5$ (between 2 and 150 keV) for a Shakura-Sunyaev disk (e.g., Fig. 1 in Yang et al. 2007; Cao 2009), and variations in f_c can change the ionizing luminosity by ~ 0.3 dex. By contrast, Figure 2 shows that variations in a (from $a = 0.998$ to -1) causes L_{ion} to vary by $\gtrsim 0.5 - 2$ dex for $\dot{m} \lesssim 0.5$ and $M_\bullet = 10^8 - 10^{10} M_\odot$ (except for $M_\bullet \lesssim 10^8 M_\odot$; see Fig. 2), respectively. The spin strongly influences the ionizing luminosity, especially when \dot{m} is decreased. Therefore, the current approach does not apply to less massive BHs with high accretion rates, such as narrow-line Seyfert 1 galaxies. Hot electron scattering of the disk surface may additionally modify the SED, but this influence does not exceed a factor of 2 (e.g., Czerny & Elvis 1987) and is neglected in the present paper. Here we focus on first-order constraints on BH spin that can be derived from $\text{H}\beta$ reverberation. More detailed measurements of the BH spin will require a need more careful treatment of the disk-corona radiation and determination of

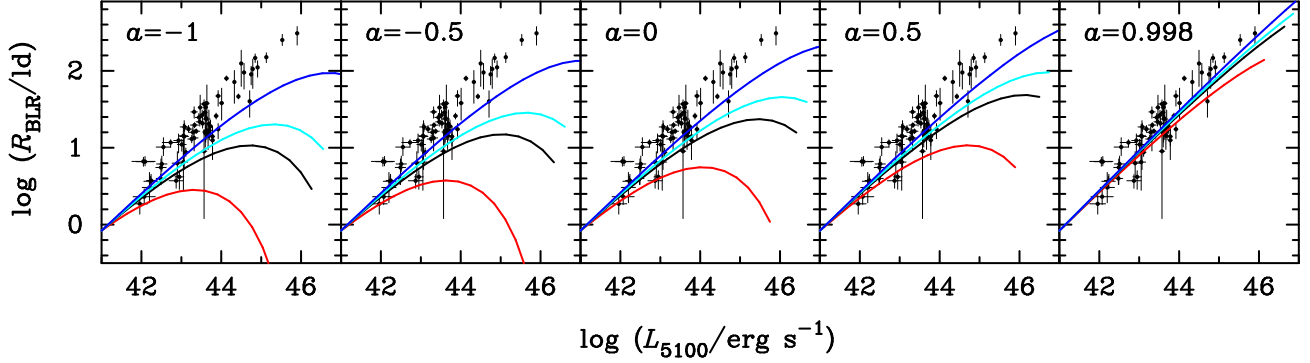


FIG. 4.— Relation between the BLR lag and the luminosity at 5100 Å. Panels from left to right are for different values of BH spin, from $a = -1.0$ to $a = 0.998$. Each panel plots four colour lines for different accretion rates. The normalization constants, for $\dot{m} = (0.01, 0.05, 0.1, 0.5)$, are as follows: $a = -1$: $R_0 = (18.4, 12.0, 10.6, 8.4)$ ld; $a = -0.5$: $R_0 = (16.3, 11.2, 10.0, 8.2)$ ld; $a = 0$: $R_0 = (14.2, 10.3, 9.4, 7.9)$ ld; $a = 0.5$: $R_0 = (12.0, 9.3, 8.6, 7.5)$ ld; and $a = 0.998$: $R_0 = (8.3, 7.4, 7.2, 6.6)$ ld.

the parameter $n_e U$ from photoionization calculations.

2.3. Size-luminosity Relation

The strong empirical correlation $R_{\text{BLR}} \approx 33 L_{44}^{\gamma} \text{ ld}$ (Bentz et al. 2013) is in good agreement with the constant- $n_e U$ model. L_{5100} can be converted into L_{ion} for a given accretion disk model. We calculate the $R_{\text{BLR}} - L_{5100}$ relation by inserting $L_{\text{ion}} = \ell L_{5100}$ into the constant- U model. Supposing that $R_{\text{BLR}} \propto L_{\text{ion}}^{\gamma} = \ell^{\gamma} L_{5100}^{\gamma}$, we have $R_{\text{BLR}} = R_0 \ell^{\gamma} L_{44}^{\gamma}$, where $R_0 = 36.3/\ell_0^{\gamma}$ is the normalization, and ℓ_0 is ℓ obtained by setting $L_{5100} = 10^{41} \text{ erg s}^{-1}$ for given a and \dot{m} .

Figure 4 shows the photoionization-based model of the variation of BLR size with L_{5100} . The normalization is determined by the observed relation. The data of points in the plot are taken from Bentz et al. (2013). For retrograde spins ($a = -1$), the predicted time lags are generally shorter than the observed values unless the accretion rates are very high (up to the super-Eddington regime of slim disks with $\dot{m} \gtrsim 1.0$). Increasing the BH spin increases the lags and brings them into better agreement with the observed values. This is a consequence of the increased production of ionizing photons for larger values of \dot{m} and a , which leads to expansion of the ionizing front of BLR clouds and thus longer lags.

BHs with spins $a \leq 0$ lead to BLR sizes much smaller than those observed in the $R_{\text{BLR}} - L_{5100}$ relation. The sizes can be increased by elevating the accretion rates in the Shakura-Sunyaev regime, but they are still systematically too small. The only way to reconcile this discrepancy with the observed $R_{\text{BLR}} - L_{5100}$ relation is to increase the BH spin. As described in Section 3.1, there are five RM AGNs with BH spins determined through *Suzaku* observations. They are all fast-rotating BHs, and they are all consistent with the last panel ($a = 0.998$) in Figure 4. We deduce that most of the ~ 50 RM AGNs are rotating maximally.

This work shows that BHs undergoing retrograde accretion can produce $H\beta$ lags much shorter than those observed on the $R_{\text{BLR}} - L_{5100}$ relation. Self-shadowing effects from a slim disk (Wang et al. 2014), if present, further shorten the lags. Since slim disks emit a distinctive SED (Wang et al. 2014), the two effects can, in principle, be disentangled. The $R_{\text{BLR}} - L_{5100}$ relation of the current sample of RM AGNs already has a remarkably tight of 0.13 dex (Bentz et al. 2013). Some of the scatter surely must arise from variations in accretion rate and physical conditions of the BLR. Thus, barring strong selection effects of some kind, the tight observed $R_{\text{BLR}} - L_{5100}$ re-

lation strongly suggests that the current sample of RM AGNs statistically have high BH spins. By the same token, future, larger RM samples provide an opportunity to discover BHs with low or even retrograde spins by identifying outliers in the $R_{\text{BLR}} - L_{5100}$ relation.

2.4. FWHM and Luminosity Plane

The virial velocity of the clouds in the BLR is given by

$$V_{\text{vir}} = c/\sqrt{r_{\text{BLR}}} = 9.9 \times 10^3 \ell_{10}^{-0.27} M_8^{1/2} L_{44}^{-0.27} \text{ km s}^{-1}, \quad (7)$$

where $r_{\text{BLR}} = R_{\text{BLR}}/R_g$ is the BLR size in units of R_g , $\ell_{10} = \ell/10$, and $M_8 = M_{\bullet}/10^8 M_{\odot}$. Since ℓ is a function of $(M_{\bullet}, \dot{m}, a)$, the plane formed by the two observables FWHM and L_{5100} can deliver information on the spin.

We plot the RM AGNs as red points in Figure 5; they are quite homogeneously distributed in the FWHM- L_{5100} plane. As shown by the panels, the distribution of RM AGNs is mostly covered by model lines that cover $\dot{m} \in (0.1, 0.5)$ and $a = 0.998$. We also show the quasar sample from Hu et al. (2008). Interestingly most quasars occupy the region of parameter space $\dot{m} \in (0.1, 0.5)$, in general agreement with the observed Eddington ratio distribution of Sloan Digital Sky Survey quasars (e.g., Shen et al. 2011), and $a = 0.5$.

3. DISCUSSION AND SUMMARY

Measurements of BH spins are elusive in AGNs. The iron $K\alpha$ line profile, broadened and skewed by the strong gravity around the BH, is usually employed to estimate the spin of the hole (e.g., Fabian et al. 2000; Risaliti et al. 2013; see Reynolds 2013 for review). A significant fraction of the AGNs with robust constraints on their spin from X-ray observations with *XMM-Newton*, *Suzaku*, and *NuSTAR* have spin parameters $a > 0.5$ (Reynolds 2013). Among these, five have been monitored by RM. *Suzaku* observations (Walton et al. 2013) report high spins: $a = 0.86$ (Mrk 509), 0.83 (Mrk 335), > 0.64 (Fairall 9), > 0.81 (Ark 120), and > 0.99 (Ark 110). In principle, BH spins for AGNs can also be obtained from fitting the continuum with disk models (Czerny et al. 2011; Done et al. 2013), but it is often challenging to measure the full SED simultaneously. More statistical techniques rely on estimating the average radiative efficiency of AGN populations, and using this information to infer the implied BH spin and its evolution with redshift (e.g., Wang et al. 2009; Li et al. 2012; Volonteri et al. 2013).

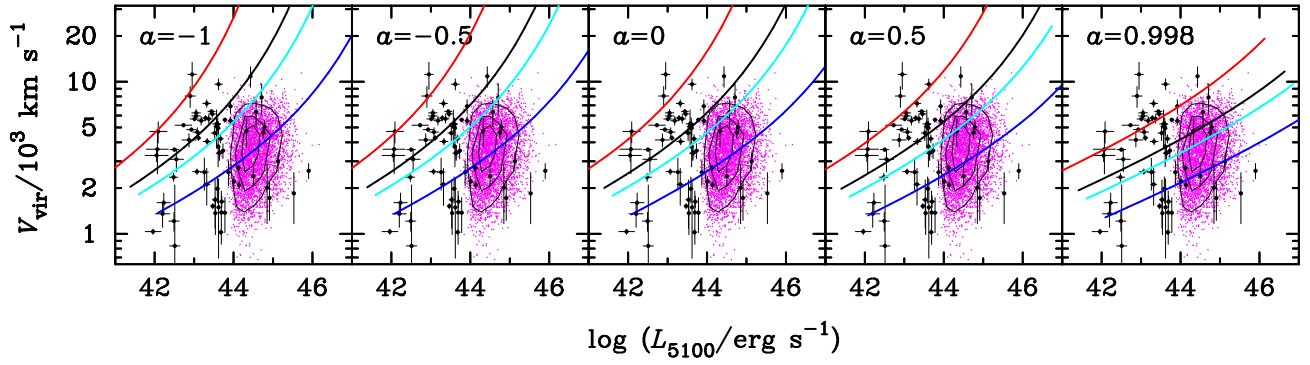


FIG. 5.— The distribution of virial velocities for the BLR clouds as a function of optical continuum luminosity. Panels from left to right are for different values of BH spin, from $a = -1.0$ to $a = 0.998$. Each panel plots four curves for different \dot{m} (corresponding to the same color). The black points are the RM AGNs, the magenta points SDSS quasars from Hu et al. (2008). The contours mark 20%, 50%, and 80% of the sample. The regions of the diagram not occupied by the quasar sample may represent massive BHs and accretion rates $\dot{m} \gtrsim 0.5$, where the present approach does not apply.

This paper offers a new approach to measure BH spins in AGNs using RM of the $H\beta$ line. Studying the BLR size-luminosity relation based on a standard accretion disk model, we find that the BLR size is very sensitive to the spin of the BH. BHs with low spins or retrograde accretion exhibit significantly shorter $H\beta$ lags in response to the varying optical continuum. In practice, our technique can be applied as follows. Using RM observations, we can derive the BH mass $M_\bullet = f_{\text{BLR}} R_{\text{BLR}} V_{H\beta}^2 / G$, where the virial factor f_{BLR} can be obtained from calibrations against the local scaling relations between BH mass and bulge properties (e.g., Onken et al. 2004; Ho & Kim 2014) or from more sophisticated dynamical models of the BLR (Pancoast et al. 2011; Li et al. 2013). As shown in Figure 2, the optical part of the disk continuum is insensitive to the spin, allowing us to estimate the accretion rates \dot{M}_\bullet . Then, invoking Figure 4, we can estimate the spin from the $R_{\text{BLR}} - L_{5100}$ relation. Applying this technique to the currently available sample of ~ 50 RM AGNs, we find that the majority of them are consistent with having fast-rotating BHs.

Apart from the $R_{\text{BLR}} - L_{5100}$ relation, we also discuss how BH spins can be constrained from the distribution of broad $H\beta$ line widths and optical luminosity (Fig. 5). The sample of $z \lesssim 0.8$ quasars from Hu et al. (2008) appears to have moderate spins ($a \approx 0.5$), qualitatively consistent with the results from Wang et al. (2009), Li et al. (2012) and Volonteri et al. (2013) based on radiative efficiency considerations. Spin parameters in the range $a = (0.5, 0.7)$ correspond to $\eta = (0.08, 0.1)$.

High-luminosity quasars are normally difficult to study through RM because of their low level of variability, pre-

dicted long variability timescales, as well as $(1+z)$ time dilution (e.g., Kaspi et al. 2007). If high- z quasars follow the local size-luminosity relation, the $H\beta$ lags are predicted to be $380(1+z)L_{46}^\gamma$ days, for $L_{46} = L_{5100}/10^{46} \text{ erg s}^{-1}$. From the results of this study, we note that the observed L_{5100} is linearly proportional to L_{ion} only for $M_\bullet \lesssim 10^8 M_\odot$. L_{ion} drops dramatically for BHs with very high mass and luminosity, which in turn leads to much shorter lags for the emission-line response. Estimating from Figure 4, a $10^9 M_\odot$ quasar with $0.2L_{\text{Edd}}$ will have its lag reduced to $\sim 20, 50$, and 200 days if $a = -1, 0$, and 0.998 , respectively. If BHs grow through random accretion (Wang et al. 2009; Li et al. 2012; Volonteri et al. 2013), some of them must undergo retrograde accretion and thus should have very short $H\beta$ lags. This expectation can be tested with future large-scale RM surveys. Additional candidates of BH with retrograde spins can be selected from luminous quasars with very broad $H\beta$ profile in the $\text{FWHM} - L_{5100}$ plane (Fig. 5).

The authors thank the anonymous referee for a helpful report clarifying several points. We are grateful to the members of IHEP AGN group for stimulating discussions. This research is supported by the Strategic Priority Research Program – The Emergence of Cosmological Structures of the Chinese Academy of Sciences, Grant No. XDB09000000, by NSFC grants NSFC-11173023, NSFC-11133006, and NSFC-11233003, and by Israel-China ISF-NSFC grant 83/13. LCH receives support from the Kavli Foundation and Peking University.

REFERENCES

- Abramowicz, M. A., Czerny, B., Lasota, J.-P., & Szuszkiewicz, E. 1988, *ApJ*, 332, 646
- Bentz, M. C., Denney, K. D., Grier, C. J., et al. 2013, *ApJ*, 767, 149
- Blandford, R. D., & McKee, C. F. 1982, *ApJ*, 255, 419
- Cao, X. 2009, *MNRAS*, 394, 207
- Czerny, B., Hryniewicz, K., Nikolajuk, M., & Sadowski, A. 2011, *MNRAS*, 415, 2942
- Czerny, B. & Elvis, M. 1987, *ApJ*, 321, 305
- Done, C., Jin, C., Middleton, M., & Ward, M. 2013, *MNRAS*, 434, 1955
- Greene, J. E., & Ho, L. C. 2005, *ApJ*, 630, 122
- Haardt, F. & Maraschi, L. 1991, *ApJ*, 380, L51
- Ho, L. C. 2008, *ARA&A*, 46, 475
- Ho, L. C., & Kim, M. 2014, *ApJ*, 789, 17
- Hu, C., Wang, J.-M., Ho, L. C., et al. 2008, *ApJ*, 687, 78
- Kaspi, S., Brandt, W. N., Maoz, D., et al. 2007, *ApJ*, 659, 997
- Kaspi, S., Smith, P. S., Netzer, H., et al. 2000, *ApJ*, 533, 631
- Laor, A., & Davis, S. 2011, *MNRAS*, 417, 681
- Li, Y.-R., Wang, J.-M., & Ho, L. C. 2012, *ApJ*, 749, 187
- Li, Y.-R., Wang, J.-M., Ho, L. C., Du, P., & Bai, J.-M. 2013, *ApJ*, 779, 110
- Merloni, A. & Fabian, A. C. 2002, *MNRAS*, 332, 165
- Negrete, C. A., Dultzin, D., Marziani, P. & Sulentic, J. W. 2013, *ApJ*, 771, 31
- Netzer, H., & Laor, A. 1993, *ApJ*, 404, L51
- Onken, C. A., Ferrarese, L., Merritt, D., et al. 2004, *ApJ*, 615, 645
- Osterbrock, D. 1989, *Astrophysics of Gaseous Nebulae and Active Galactic Nuclei* (Berkeley: University of California Press)
- Osterbrock, D. E., & Mathews, W. G. 1986, *ARA&A*, 24, 171
- Page, D. N., & Thorne, K. S. 1974, *ApJ*, 191, 499
- Pancoast, A., Brewer, B. J., & Treu, T. 2011, *ApJ*, 730, 139
- Peterson, B. M., Ferrarese, L., Gilbert, K. M., et al. 2004, *ApJ*, 613, 682
- Reynolds, C. S. 2013, *CQGra*, 30, 4004
- Risaliti, G., Harrison, F. A., Madsen, K. K., et al. 2013, *Nature*, 494, 449

- Shakura, N. I., & Sunyaev, R. 1973, A&A, 24, 337
- Shen, Y., Richards, G. T., Strauss, M. A., et al. 2011, ApJS, 194, 45
- Shuder, J. M. 1981, ApJ, 244, 12
- Svensson, R. & Zdziarski, A. 1994, ApJ, 436, 599
- Uzdensky, D. A. 2013, ApJ, 775, 103
- Volonteri, M., Sikora, M., Lasota, J.-P., & Merloni, A. 2013, ApJ, 775, 94
- Walton, D. J., Nardini, E., Fabian, A. C., Gallo, L. C., & Reis, R. C. 2013, MNRAS, 428, 2901
- Wang, J.-M., Hu, C., Li, Y.-R., et al. 2009, ApJ, 697, L141
- Wang, J.-M., Qiu, J., Du, P., & Ho, L. C. 2014, ApJ, submitted
- Wang, J.-M., Watarai, K.-Y., & Mineshige, S. 2004, ApJ, 607, L107
- Yang, F., Hu, C., Chen, Y.-M. & Wang, J.-M. 2007, ChJA&A, 7, 353